RSC Advances

PAPER

View Article Online
View Journal | View Issue

Cite this: *RSC Adv.*, 2026, **16**, 17470

Another Au_{32} gold fullerene: a novel spherical cage cluster with octahedral symmetry

Jiayu Li, Silei Wang, Jing Tian, Xiaoxia Yang, Xiaxi Lei, Lengzhang Xu, Wenwu Xu and Xiao Gu *

Received 4th January 2026
Accepted 2nd March 2026

DOI: 10.1039/d5ra09961g

rsc.li/rsc-advances

The discovery of C_{60} opened the window to the development of numerous fullerene clusters, with non-covalent gold clusters emerging as one of the most fascinating class. Notably, the icosahedral (I_h) Au_{32} cluster, the first reported metal fullerene, has attracted significant attention due to its high symmetry and stable hollow-cage structure. In this study, we report the discovery of a novel Au_{32} hollow-cage fullerene structure exhibiting octahedral (O_h) symmetry. This configuration demonstrates remarkable stability with a substantial HOMO–LUMO energy gap. Theoretical analysis reveals that the O_h cage can stably encapsulate up to four additional gold atoms within its framework. A systematic exploration of the O_h cage structure with all elements led to the identification of a series of stable endohedral fullerene clusters. In total, 30 stable hollow cage structures with the O_h symmetry are identified, including Au_{32}, Ag_{32}, Cu_{32}, B_{32}, and Si_{32}. This work offers insights into the cage structures of fullerene clusters and advances the fundamental understanding of all-metal-element fullerenes.

1. Introduction

Highly symmetric clusters have always been a hot topic in both theoretical and experimental studies due to their unique physicochemical properties and excellent stability. In particular, cage-like highly symmetric clusters are widely recognized for their potential in constructing functional nanomaterials. Among these, fullerene clusters, with their unique geometrical structures and excellent properties, have demonstrated a wide range of applications in various fields, such as energy storage, catalysis, optoelectronic sensing, and biomedicine.

In 1985, H. W. Kroto *et al.* successfully synthesized a molecular cluster consisting of 60 carbon atoms in a truncated icosahedral structure. The cluster had an I_h symmetry and a large π-conjugated structure, and it was a superstable species.[1] This discovery initiated in-depth studies on highly symmetric cage-like materials. Subsequently, theoretical and experimental studies predicted fullerene structures of different sizes. Fullerenes are widely used in materials chemistry and electron transport applications due to their good chemical stability and excellent electron affinity, and they can be used as precursors for fullerene derivatives.[2,3] The C_{24} fullerene cage is one of the smallest and stable fullerene structures with high thermodynamic stability and shows better stability than C_{60} in photocatalytic water decomposition.[4]

The covalent fullerene families have unsurprisingly expanded. In 2007, Nevill Gonzalez Szwacki *et al.* theoretically designed the B_{80} fullerene, which is geometrically very similar to the C_{60} fullerene, maintains an I_h symmetry, and has a relatively large HOMO–LUMO energy gap.[5,6] Subsequently, B_{180}, which consists of six crossed double-rings (DRs) with an almost perfect spherical shape, was successfully predicted, and the connection between the fullerene family and its precursors, boron sheets (BSs), was explored.[7] In addition, the stable cage structures of B_{14},[8] B_{38},[9] B_{40},[10,11] B_{48},[12] B_{50},[13] B_{56},[14] B_{100},[15] and B_{112} [16] were theoretically verified by researchers.

What really surprised the scientific society is that non-covalent, pure metal atoms could also form fullerene structures. In 2004, using the density functional theory (DFT) method, we discovered an I_h Au_{32} hollow cage-like cluster, which is the first reported all-metal-atom fullerene;[17] earlier studies have predicted a variety of possible Au_{32} structures, including icosahedral, decahedral, and close-packed.[18] Due to the unexpected all-metal cage structure, extensive and in-depth studies on the structure of Au_{32} were conducted. Subsequently, a space-filling structure (C_1) of Au_{32} was proposed and compared with a hollow cage structure (I_h), where the I_h structure was found to be more energetically stable and spherically aromatic.[19] Wei Fa *et al.* used a relativistic density-functional approach combined with the Broyden–Fletcher–Goldfarb–Shanno algorithm to propose caged Au_{32} structures with a D_{6h} symmetry as well as novel tubular gold cluster structures and discussed their unique features using the absorption spectra.[20] Using the DFT-GGA method, Jalbout *et al.* found that the low symmetry Au_{32} structure in the ionic state was preferred over the caged fullerene-like isomers. At the same time, several low-symmetry isomers (C_1) of Au_{32} were reported.[21] Johansson *et al.*

School of Physical Science and Technology, Ningbo University, Ningbo 315211, China. E-mail: guxiao@nbu.edu.cn

calculated multiple structures of Au_{32}, including a stable competing isomer "J10" (C_1) reported at that time, as well as structures with the T_h and C_{2v} symmetries. Results showed that the "J10" anion exhibited a lower energy, but for neutral and cationic states, the hollow fullerene still remained in its predominantly stable form.[22] Besides, by combining DFT with molecular dynamics simulations, Himadri Sekhar De *et al.* calculated other *C* symmetric hollow and space-filling configurations of Au_{32}, revealing the dynamic behavior of Au_{32} clusters at different temperatures and further verifying the low symmetry and temperature dependence of structures other than the I_h-symmetric one.[23] Using first-principles calculations, Baletto *et al.* identified a low-symmetry "worm"-like structure with hollow and elongated features, which is the second most stable isomer after the icosahedral fullerene cage.[24] In 2015, Zhao *et al.* used relativistic density-functional theory (RDFT) optimization methods to investigate the properties of a wide range of Au_{32} structures, including the hollow cage, tube-like, double-layered flat, face-centered cubic-like (fcc-like), and close-packed configurations.[25] Recently, Wang *et al.* analyzed the electron structures of Au_{32} nanoclusters by the same method. In addition to neutral Au_{32} hollow species, other symmetry-stabilized Au_{32} structures were calculated, such as $[Au_{32}]^{8+}$ (single-shell layered structure), $[Au_{32}]^{4+}$ (double-shell structure) and $[Au_{32}]^{2+}$ (C_1).[26] Using density-functional tight-binding (DFTB) in combination with numerical finite-difference methods, K. Vishwanathan *et al.* revealed that there also exists a low-symmetry core–shell structure for Au_{32}.[27]

In the existing literature, most Au_{32} isomers are predicted to be compact or disordered, except for the stable Au_{32} isomer with an I_h symmetry, which we was first discovered in 2004. However, for a cluster, its symmetry is often closely correlated with its stability. Typically, a structure with a stronger symmetry tends to exhibit a lower potential energy and higher stability. Therefore, exploring other stable symmetrical isomers is not only conducive to gain a deeper understanding of the relationship between the structure and properties but also to provide a theoretical basis for the development of new gold-based materials.

Through our persistent efforts and systematic research, we discovered another hollow cage-like fullerene structure of Au_{32} with an O_h symmetry. This structure demonstrates high stability in theoretical calculations, and a further analysis of its electronic structure reveals that it exhibits a relatively large energy gap between the highest occupied molecular orbital (HOMO) and the lowest unoccupied molecular orbital (LUMO). These characteristics suggest that the structure possesses good thermodynamic and chemical stability and shows significant potential in electronic applications.

2. Computational details

All calculations were performed using density functional theory (DFT) within the framework of the Vienna *ab initio* simulation package (VASP),[28] employing the generalized gradient approximation (GGA) in the Perdew–Burke–Ernzerhof (PBE) form[29] with Grimme's DFT-D3 van der Waals correction to account for long-range dispersion interactions.[30] The projector augmented wave (PAW)[31] method was utilized to accurately describe the interactions between the core and valence electrons.

A plane-wave energy cutoff of 450 eV was applied, and the force convergence criterion was 0.01 eV $Å^{-1}$. The forces acting on all unconstrained atoms were converged within 0.05 eV $Å^{-1}$. For the computations, individual clusters were placed in a cubic supercell with dimensions of $30 \times 30 \times 30$ $Å^3$. The use of large supercells ensured that the interactions between the cluster and its periodically repeated images were negligible. *K*-space sampling was performed exclusively at the gamma point.

The bonding mode of Au_{32} was elucidated *via* the adaptive natural density partitioning (AdNDP) analysis.[32] The steps required for the analysis were performed in Gaussian 16,[33] employing the B3PW91 hybrid functional and LANL2DZ basis set. The analysis of AdNDP delocalized orbitals was conducted in the Multiwfn software.[34,35]

3. Results and discussion

Gold clusters exhibit interesting and important electronic, optical, chemical, and catalytic properties, which rely on their diverse geometric structures.[36–38] In 2003, Jun Li *et al.* discovered a tetrahedral (T_d) structure, Au_{20}, which showed a theoretically and experimentally stable structure with a large HOMO–LUMO energy gap.[39] In this T_d pyramid Au_{20}, all the gold atoms were present on the surface. The discovery of T_d Au_{20} and I_h Au_{32} formally opened up the exploration of all-gold fullerene structures. Au_{42}, which was constructed based on a C_{80} fullerene template, could form a perfect icosahedral structure with an I_h symmetry; its diameter was about 1.1 nm, which was 0.2 nm larger than that of the Au_{32} fullerene, and could accommodate up to 13 Au atoms.[40] Muñoz-Castro *et al.* reported a high-energy D_{6h}-symmetric isomer of Au_{42}, which exhibited novel superatomic π-orbital characteristics and followed the Hirsch's rule for spherical aromaticity; it serves as a typical example that facilitates the exploration of structure–property relationships through non-global minimum structures.[41] Satya Bulusu *et al.* experimentally confirmed the existence of hollow cage structures in Au_{16}^-, Au_{17}^- and Au_{18}^- gold anion clusters, and these structures exhibited diameters larger than 5.5 Å, conducive for the easy accommodation of a guest atom.[42] Au_{34}^- has a chiral structure with C_3 point symmetry, which has been shown to be its most stable structure both theoretically and experimentally.[43] Au_{50} exhibited a cage-like structure with a D_{6d} symmetry, a larger HOMO–LUMO gap (1.072 eV) and spherical aromaticity.[44] Jacobo-Fernándeza *et al.* performed a DFT-D study on neutral and charged Au_{60} clusters, and they found that the neutral structure featured an *I*-symmetry (hollow structure), while the structures with 1^-, 1^+, and 2^+ charge states featured a C_s symmetry.[45] The Au_{72} cluster with *I* symmetry is a hollow gold cage with spherical aromaticity and high thermodynamic stability, which could function as a chiral catalyst in catalytically active small gold nanostructures.[46] Large-size cage structures of Au_{92} and Au_{122} constructed based on the icosahedral template approach, exhibit good I_h symmetry and are energetically stable.[47] In addition to planar and hollow cage structures, the

double shell structure is an important candidate structure for gold clusters. Au_{58} is a typical example, in which the inner shell consists of 10 atoms, and it forms a hollow structure and exhibits high stability.[48] Among all the structures mentioned above, the Au_{32} fullerene with an I_h symmetry is the unique cluster.[49] Tlahuice-Flores proposed the polyhedron approach, which takes tetrahedra and octahedra as basic structural units and systematically reveals the structural characteristics of thiolate-protected gold clusters as well as their size-dependent evolution rules through the assembly modes of sharing vertices, edges or faces. Using this mechanism, an I_h-symmetric Au_{32} could be formed, with one icosahedron surrounded by 20 octahedral blocks, which is structurally isomorphic to I_h-Au_{32}.[50]

Recently, we developed a novel method for constructing highly symmetrical structures based on a conjugate-dual structure.[51] A conjugate-dual structure is formed by combining a polyhedron with its corresponding dual polyhedron. The dual polyhedron is obtained by replacing each face of the original polyhedron with a vertex and each vertex with a face. To ensure that the combined structure shares the same center and the face–vertex pairs are conjugately aligned, the vertices of the dual polyhedron are aligned with the face centers of the original, and the face centres of the dual polyhedron are aligned with the vertices of the original. This approach preserves or enhances the original polyhedron's symmetry, leading to a new family of clusters. Surprisingly, in the structural exploration of conjugate-dual structures, rather than the I_h Au_{32} fullerene, we discovered another Au_{32} fullerene with an O_h symmetry.

To identify the potential isomers and explore other possible structures of Au_{32}, we employed ABCluster for structural searches.[52] This method involves randomly placing points within a 30 × 30 × 30 $Å^3$ unit cell and performing global optimization to identify the stable structures of Au_{32}. Results provided various potential structural forms (*e.g.*, cage-like or space-filling), which were further optimized in our DFT calculations.

Fig. 1 displays the isomers of the Au_{32} cluster obtained from the above calculations, labeled as isomers I to VIII. It shows that only isomers I and II are symmetric, possessing the I_h and O_h symmetries, respectively. All the other isomers are asymmetric, which belong to the C_1 point group and are characterized as amorphous; these isomers are ordered according to the decreasing order of total energy from III to VIII. These asymmetric 3D structures are more compact and can be viewed as distorted cages embedded with 1 to 3 gold atoms.

Table 1 lists symmetry, radius, total energy, and HOMO–LUMO gap for the isomers of Au_{32}. Isomers I is the dual structure of C_{60} with an I_h symmetry, presenting a stable icosahedral structure formed by encapsulating one Au atom at each pentagonal face, with bond lengths of 2.74 Å and 2.83 Å, which are consistent with previous studies.[17] Isomers III and IV represent two other hollow configurations, with isomers III being slightly more stable than isomer IV in terms of energy. For the Au_{32} cage containing gold atoms, isomers V and VI each have 1 and 2 gold atoms embedded internally, while isomers VII and VIII contain 3 gold atoms inside.

We systematically optimized and calculated the properties of Au_{32} in five charge states (Au_{32}^{2-}, Au_{32}^{1-}, Au_{32}^{0}, Au_{32}^{1+}, and Au_{32}^{2+}). As the negative charge increases, the relative total energy decreases (Tables S1–S4), which is consistent with the high electronegativity of Au atoms and aligns well with the photoelectron spectroscopy (PES) experimental results for anionic Au_{32} clusters reported by Ji *et al.*[53] For all the four charged states considered (±1 and ±2), the global minimum structures of Au_{32} are found to be of low-symmetry C_1

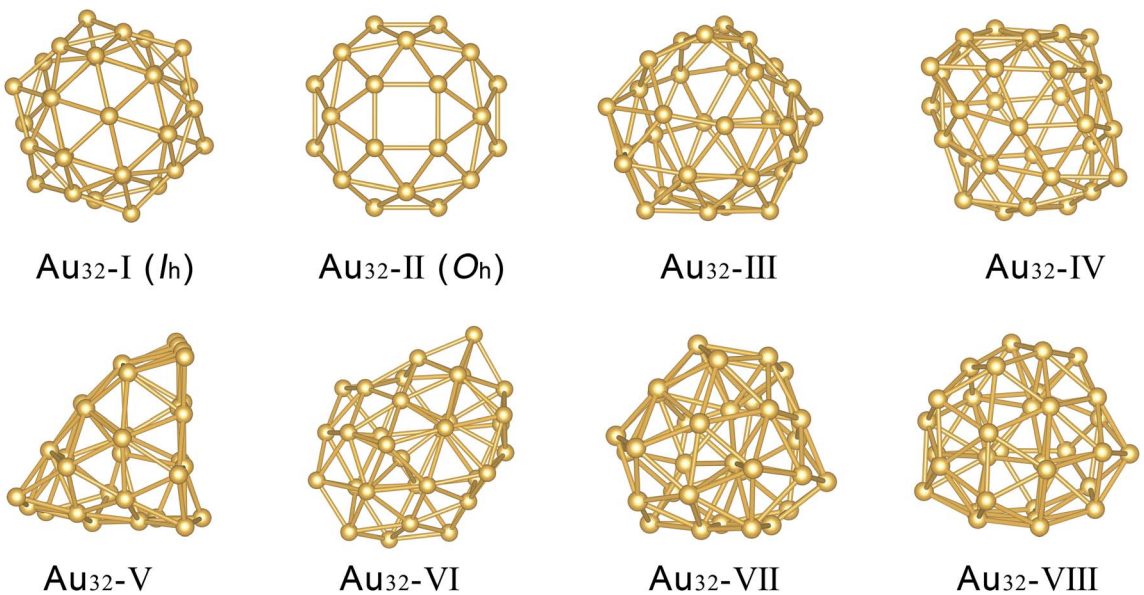

Fig. 1 Au_{32} cluster isomers obtained *via* DFT structural optimization. Au_{32}-I: cage-structure with an I_h symmetry. Au_{32}-II: cage-structure with an O_h symmetry. Au_{32}-III to Au_{32}-VIII: asymmetric isomers (belonging to the C_1 point group), where isomers III and IV are hollow structures, isomer V contains one gold atom inside, isomer VI contains two gold atoms inside, and isomers VII and VIII contain three gold atoms.

Table 1 Properties of the eight isomers presented in Fig. 1. The radius is the distance from the center of the sphere to the farthest placed Au atom. The total energy of each fullerene is presented relative to that of $Au_{32}^{0}(I_h)$

Isomer	Symmetry	Radius (Å)	Total energy (eV)	HOMO–LUMO gap (eV)
I	I_h	4.47	0	1.56
II	O_h	4.28	0.76	1.58
III	C_1	4.71	1.05	0.89
IV	C_1	5.15	1.18	0.44
V	C_1	5.85	2.02	0.32
VI	C_1	5.25	−0.29	0.22
VII	C_1	4.29	−0.71	0.37
VIII	C_1	4.37	−0.99	0.34

configurations. This finding verifies the principle that cluster systems can achieve lower total energy at the cost of partial symmetry reduction, which is fully consistent with the classic studies on charged Au_{32} clusters by Abraham F. Jalbout *et al.*[21] From the perspective of electronic structure, high-symmetry isomers exhibit larger HOMO–LUMO gaps compared with their low-symmetry C_1 counterparts at the same charge state. Conversely, most low-symmetry C_1 isomers exhibit narrow or vanishing gaps, which is the characteristic of a metallic behavior.

It is particularly noteworthy that we discovered a novel and highly stable Au_{32} hollow-cage fullerene structure, which is shown as isomer II in Fig. 1. Specifically, the left side of Fig. 2(a) depicts a truncated octahedron with octahedral symmetry (yellow). By selecting the vertices at the centers of the eight hexagonal faces and connecting them, a cube is formed (blue). Then, by combining the truncated octahedron with the cube under the conditions of coincident centers and equal radii, we obtained a conjugated dual hollow cage-like structure with 32 vertices and an O_h symmetry. This O_h structure shows an interesting correlation with truncated octahedral Cu_{38} clusters reported in previous studies.[18,54–56] The O_h-Au_{32} structure can be considered structurally analogous to the Cu_{38} cluster, in which the central six atoms have been eliminated and only the outer framework remains intact. Notably, the six atoms inside the Cu_{38} cluster could be located outside the structure to obtain an Au_{38} structure, as shown in Fig. S1(a).

Fig. 2 presents the structural details of the O_h Au_{32} isomer, with color codes provided for the different types of vertices. The 32 gold atoms are evenly distributed across 24 five-coordinate sites and 8 six-coordinate sites, corresponding to the yellow and blue regions in the figure, respectively.

The optimized structure retains the six quadruply bonded rings (squares) and exhibits excellent stability, which is relatively rare for hollow cage structures. In the O_h Au_{32} cage, the structure is formed by encapsulating one Au atom at the center of each hexagonal face, resulting in two distinct types of vertices: 24 five-coordinate points and 8 six-coordinate points. There are only two different bond lengths: (i) 2.70 Å—for the bond shared between the quadruply bonded ring and the hexagonal ring and (ii) 2.79 Å—for the bond between the central atom in the hexagonal ring and the six atoms on the ring. The bond angles are 90°, 58°, and 61°, all of which indicate that the optimized dual points remain well-positioned at the original hexagonal face centers.

Au_{32} is a closed-shell molecule with a significant HOMO–LUMO gap, which is an important factor for its stability. The I_h Au_{32} cluster, due to its high symmetry, has been shown[17] to possess a very large HOMO–LUMO gap of 1.558 eV, which is consistent with our computed value of 1.56 eV. The O_h cage discovered in this study also exhibits a similar HOMO–LUMO

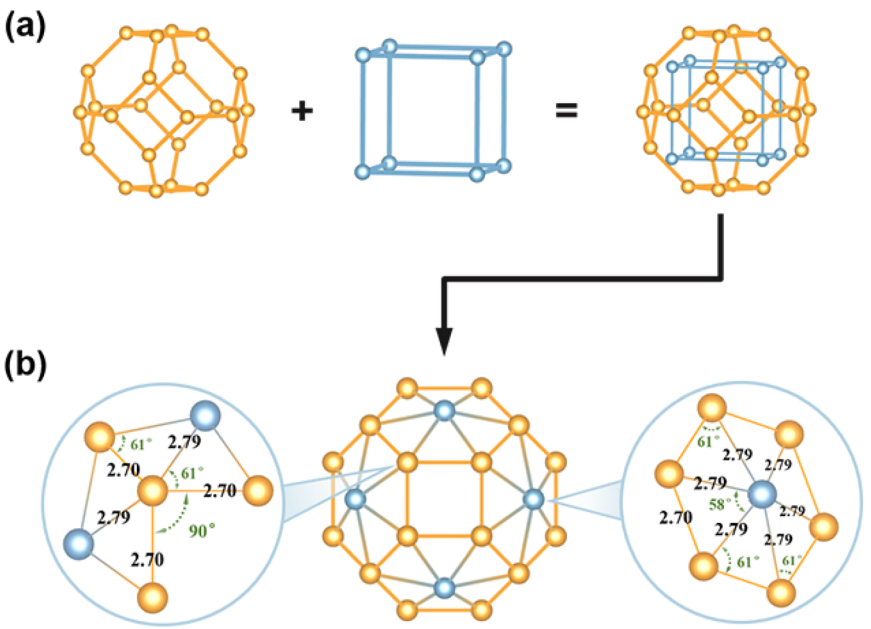

Fig. 2 (a) Conjugate combination of the gold O_h Au_{32} fullerene (co-dual structure with one truncated octahedron and one cube). (b) Structural details of the O_h isomer of Au_{32}, with vertices colored according to the coordination number.

gap of 1.58 eV. In general, molecules with a larger HOMO–LUMO gap are more stable, and thus, from a kinetic perspective, such a HOMO–LUMO gap suggests that O_h-Au_{32} is chemically very inert. Other isomers listed in this study either have no HOMO–LUMO gap or only a small gap of 0.6 ± 0.3 eV.

In Fig. 3, we show the HOMO and LUMO orbitals of the I_h and O_h cages of Au_{32}. For both the cages, the HOMO and LUMO exhibit some delocalization, spreading across the entire cluster space. Additionally, for the lower-energy I_h cage, both the HOMO and LUMO are fourfold-degenerate. For the O_h cage, the LUMO is non-degenerate, while the HOMO is three folded generate, with another triply degenerate molecular orbital located 0.155 eV below the HOMO.

The population analysis of the O_h cage reveals the average numbers of s, p, and d electrons to be 0.59, 0.21, and 8.80, respectively. This data indicate that some electrons have shifted from the d orbitals to the s and p orbitals when compared with the original $s^1p^0d^{10}$ electron configuration of the isolated Au atoms. In previous studies, Gong and his colleagues suggested that relativistic effects lead to strong s–d hybridization, which appears to explain the stability of the gold cluster cage structures.[53]

We calculated the vibrational frequencies of the clusters, with all results depicted in Fig. S2. For the I_h-Au_{32} cluster, the calculated vibrational frequencies lie between 32 and 149 cm^{-1}. Similarly, the vibrational frequency range of the O_h-Au_{32} cluster is approximately 14 to 154 cm^{-1}, with specific values listed in Table S1.

The molecular dynamics simulations reveal that the Au_{32} with an O_h symmetry exhibits remarkable thermal and structural stability at 300 K. Through a 4 ps *NVT* ensemble simulation, it was observed that the total energy of the system fluctuates stably around approximately −90.92 eV, demonstrating that the cluster maintains a stable thermodynamic equilibrium at this temperature. Crucially, the final configuration obtained after the simulation shows no significant structural reconstruction or symmetry breaking compared with the initial highly symmetric O_h geometry. These findings provide important theoretical evidence for the potential application of Au_{32} in room-temperature environments, such as in catalysis or sensing, where its structural integrity is essential.

To further confirm aromaticity, adaptive natural density partitioning (AdNDP) analysis was employed. The AdNDP analysis for Au_{32} shows a typical layered electronic structure composed of localized lone-pair electrons and globally delocalized bonds. 5d orbitals of Au atoms has been fully occupied, which form five pairs of localized lone-pair electrons. These electrons correspond to 160 1c–2e bonds. They only stabilize atomic cores and do not participate in cluster skeleton bonding or electron delocalization.

After excluding the localized electrons, the remaining 32 valence electrons are uniformly distributed in 16 delocalized 32c–2e bonds. These orbitals constitute a globally delocalized electron system inside the cluster cage. The crystal field effect of the O_h-symmetric field induces an energy level splitting of the superatomic shells. The orbital degeneracy presents a non-degenerate feature with the values of 1, 3, 3, 3, and 6. However, the total number of orbitals and electron occupancy still strictly follow Hirsch's rule for spherical aromaticity [the $2(n+1)^2$ rule, $n = 3$]. They correspond to the $1S^21P^61D^{10}1F^{14}$ superatomic electronic shell configuration, as shown in Fig. S3. This globally delocalized electron distribution conforms to the spherical aromaticity electron-counting rule, thereby verifying that the O_h-Au_{32} clusters possess distinct and robust spherical aromaticity.

Upon investigating the impact of embedding atoms inside hollow structures on the structure and properties of the external cage, we found that as the number of embedded gold atoms increased, the internal structure of the atomic clusters under two types of symmetry became more complex. For the icosahedral Au_{32}, when 1–3 gold atoms are embedded, the external cage structure remains largely unchanged. However, when more gold atoms are inserted into the cage, the external structure shows significant distortion and deformation. This is consistent with previously reported results.[17] For the O_h Au_{32} cage, the external structure remains stable with up to 4 embedded gold atoms, but strong distortion and deformation occur when 5 or more gold atoms are embedded. Specifically, after embedding 1 gold atom, that Au atom adsorbs at an interior site of a tetrahedral face and forms covalent bonds with the four atoms that constitute the tetrahedral face, and the optimized structure retains the O_h symmetry. When 2 gold atoms are embedded, the

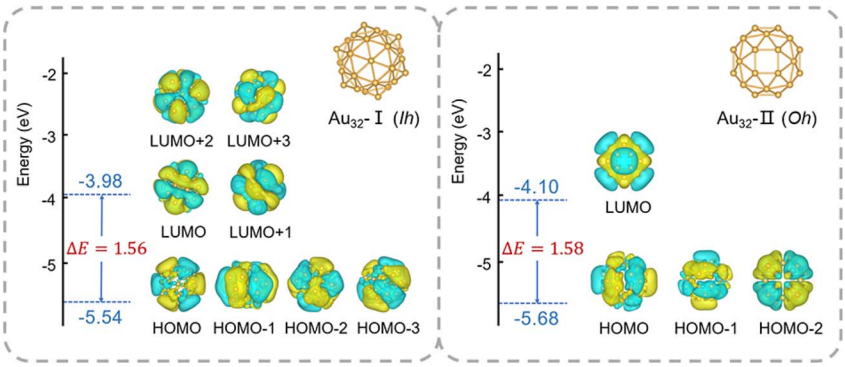

Fig. 3 Comparison of the HOMO and LUMO orbitals of the two Au_{32} fullerenes (I_h and O_h), along with the degeneracies of the HOMO and LUMO.

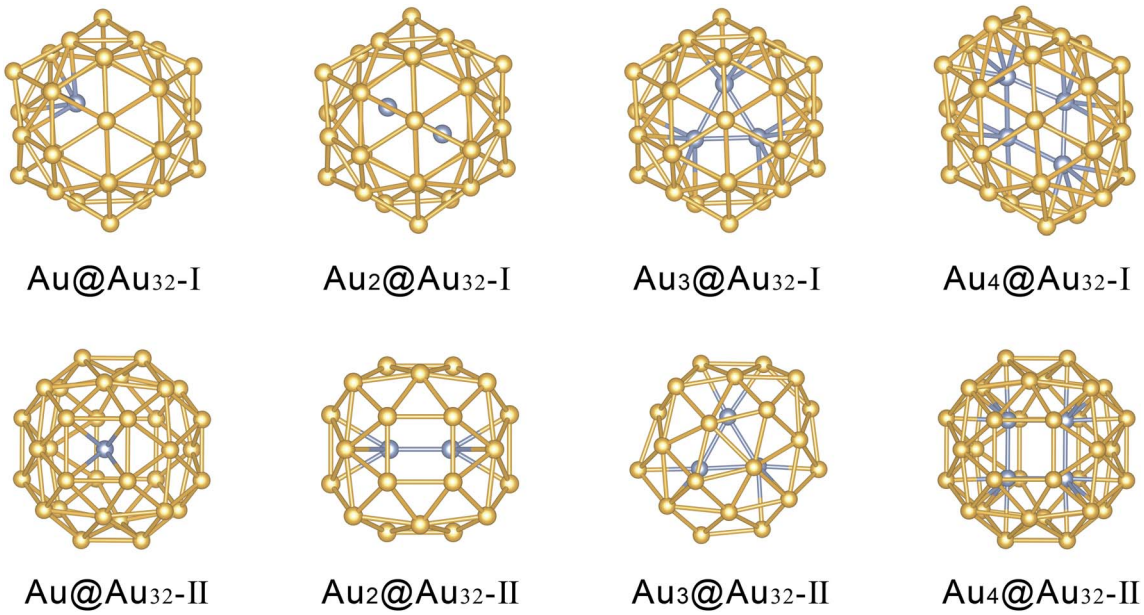

Fig. 4 Geometries of the I_h and O_h isomers upon embedding 1–4 gold atoms after DFT structural optimization, respectively. The golden atoms represent the atoms on the cage surface, while the blue atoms represent the embedded atoms.

structure degenerates to a D_{2h} symmetry, and due to the limited internal space, the gold atoms begin to form new bonds with the external cage. When the number of atoms reaches 3, they form a triangular arrangement on the ecliptic plane, reducing the symmetry to C_s. Interestingly, with the addition of the fourth atom, the symmetry increases to D_{4h}, and the four atoms form a square arrangement similar to that of the external shell. Fig. 4 shows the relaxed structures of the I_h and O_h isomers upon embedding 1–4 gold atoms.

Additionally, as the number of embedded gold atoms increases, the energy of the atomic cluster systems under both symmetries gradually decreases, indicating that the structure becomes more stable energetically. Regarding the energy gap, the I_h symmetry Au_{32} atomic cluster shows a decrease in the HOMO–LUMO energy gap as the number of embedded gold atoms increases, while the O_h symmetry Au_{32} atomic cluster exhibits a non-monotonic trend, with more complex changes in the HOMO–LUMO energy gap. From the perspective of energy and radius changes, embedding gold atoms enhances the structural stability but may sacrifice some electronic properties, such as the reduction in the energy gap. This reduction may imply an increase in the chemical reactivity of the atomic cluster as a lower HOMO–LUMO energy gap is generally associated with higher reactivity. These changes could have significant implications for the application of atomic clusters in fields such as catalysis or electronics (Table 2).

The hollow structure of Au_{32} gold fullerenes exhibit clear practical application potential in multiple fields due to their stable cage-like structure, tunable electronic properties, and good modifiability: in the biomedical field, it can form stable complexes through functionalization with amino acids such as glycine and cysteine. With high biocompatibility and structural stability, they could serve as novel drug carriers, avoiding premature drug release at room temperature and providing support for the targeted delivery of small-molecule chemotherapeutic drugs.[58] Meanwhile, the Au_{32}^{8+} nanocluster is the first ligand-protected gold fullerene synthesized according to wet chemistry. Its stable $Au_{12}@Au_{20}$ core, co-protected by phosphine and dipyridylamido ligands, serves as a precise structural template for fabricating functionalized gold

Table 2 Properties of the eight structures presented in Fig. 4. The radius is the distance from the center of the sphere to the farthest placed Au atom. The total energy of each fullerene is presented relative to that of $Au_{32}^{0}(I_h)$

Structure of cage	Number of atoms inside	Symmetry	Radius (Å)	Total energy (eV)	HOMO–LUMO gap (eV)
Au_{32}-I (I_h)	1 Au	I_h	4.50	−2.85	1.50
	2 Au	C_{2h}	4.52	−7.41	1.40
	3 Au	C_1	4.53	−10.85	1.19
	4 Au	C_1	4.74	−13.95	—
Au_{32}-II (O_h)	1 Au	O_h	4.36	−1.97	1.56
	2 Au	D_{2h}	4.50	−6.64	1.08
	3 Au	C_s	4.76	−10.65	—
	4 Au	D_{4h}	4.46	−12.95	1.46

nanomaterials.[59] The Au_{32} nanocluster obtained from Au_{36} *via* phosphine-mediated structural transformation can be used in the field of catalysis. Surface reconstruction exposes active core sites, achieving a CO faradaic efficiency of 97.7% at −0.8 V *versus* RHE in electrocatalytic CO_2 reduction.[60] Future research will focus on the experimental synthesis and characterization of Au_{32}, precise control of functionalization processes, and validation of application scenarios, thereby promoting this novel all-metal fullerene from theoretical design to practical application.

Based on the theoretical investigation on the structure and stability of the O_h-symmetric hollow cage Au_{32} cluster in this work, we hypothesized that the well-established gas-phase and wet-chemical synthesis methods for I_h-symmetric Au_{32} clusters can be modified and used for the construction of the O_h Au_{32} cluster. This O_h-symmetric isomer may be controllably fabricated *via* three feasible experimental routes, namely, low-temperature gas-phase synthesis, wet-chemical preparation regulated by octahedral structure-directing ligands, and stabilization through endohedral metal doping.

The Au_{32} fullerenes exhibit two distinct symmetric structures: I_h and O_h. Previous studies have attributed the unusual stability of the Au_{32} I_h cage to the influence of spherical aromaticity, and it satisfies the $2(n+1)^2$ electron counting rule.[57] Previous studies have also shown that the O_h-symmetric B_{32} cluster is a stable isomer,[12] despite not satisfying the $2(n+1)^2$ electron counting rule. This suggests that there may be stable structures that do not strictly follow the valence electron rule. Therefore, we extended our computational screening to all relevant elements across the periodic table to systematically investigate the relationship between geometric configuration and electronic stability.

Our results reveal that multiple elements can form stable O_h-symmetric M_{32} clusters. Among them, seven clusters satisfying the $2(n+1)^2$ electron counting rule, namely, Au_{32}, Cu_{32}, Na_{32}, K_{32}, Rb_{32}, Li_{32}, and Fr_{32}, are shown in Fig. 5(a). Structural

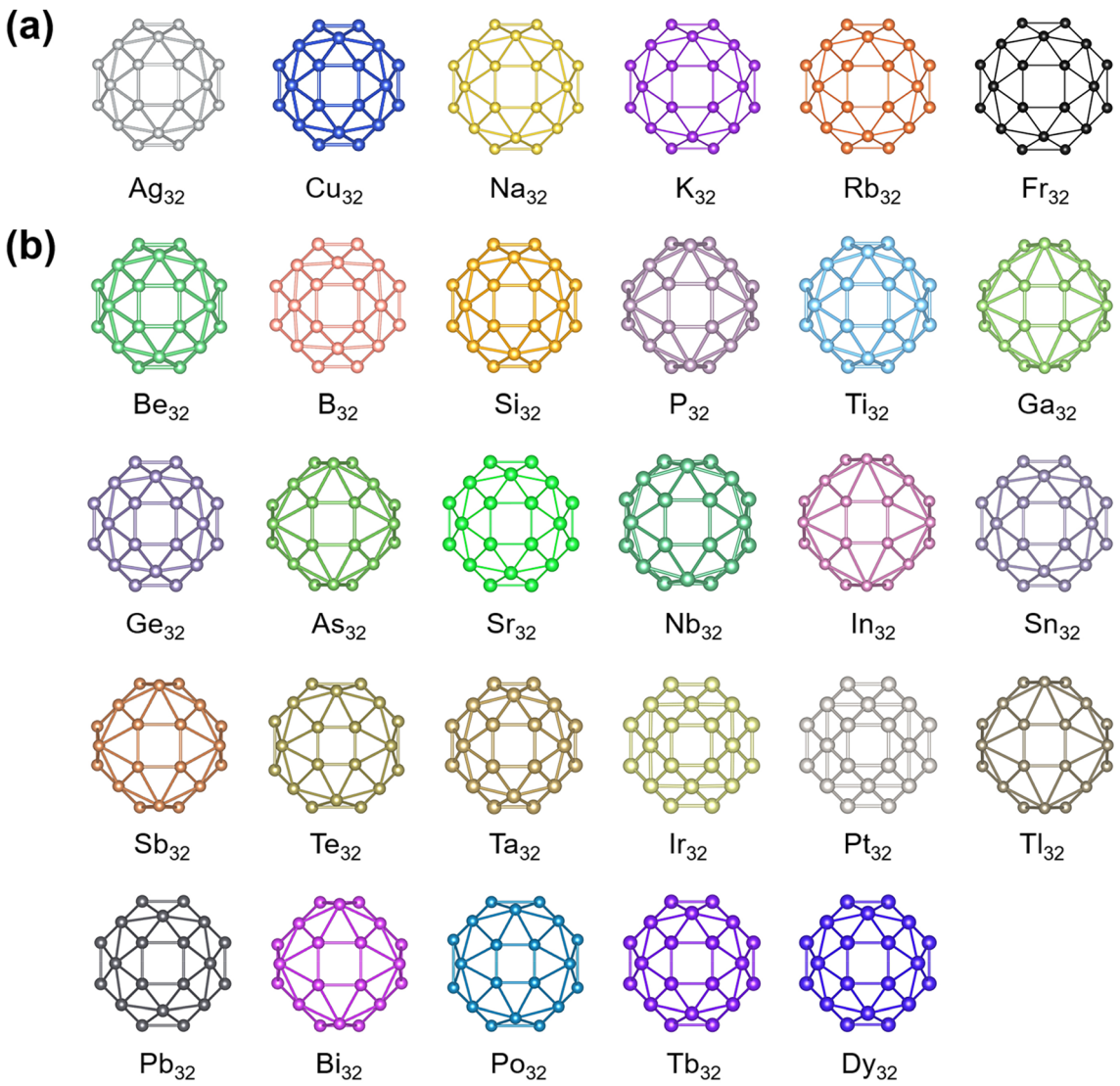

Fig. 5 Structure of the M_{32} clusters with an O_h-symmetry. (a) Stable O_h structures satisfying the $2(n+1)^2$ electron counting rule. (b) Stable O_h structures that do not satisfy the $2(n+1)^2$ electron counting rule.

Table 3 Physical and chemical properties of the stable structures presented in Fig. 5. The radius is the distance from the center of the sphere to the farthest Au atom

Cluster	Radius (Å)	Valence electron count	HOMO–LUMO gap (eV)
Ag_{32}	4.35	32	1.62
Cu_{32}	3.77	32	1.34
Na_{32}	5.52	32	0.85
K_{32}	7.05	32	0.53
Rb_{32}	7.55	32	0.47
Fr_{32}	8.29	32	0.39
Be_{32}	3.24	64	1.31
Sr_{32}	6.50	64	—
B_{32}	2.72	96	1.31
Ga_{32}	4.84	96	0.47
In_{32}	5.45	96	—
Tl_{32}	5.60	96	—
Si_{32}	3.87	128	0.38
Ti_{32}	3.98	128	—
Ge_{32}	4.26	128	—
Sn_{32}	4.88	128	0.27
Pb_{32}	5.10	128	0.71
P_{32}	4.14	160	—
As_{32}	4.67	160	—
Nb_{32}	4.14	160	—
Sb_{32}	5.25	160	—
Ta_{32}	4.16	160	—
Bi_{32}	5.50	160	—
Te_{32}	5.00	192	—
Po_{32}	5.20	192	—
Ir_{32}	4.05	288	—
Pt_{32}	4.13	320	—
Tb_{32}	5.20	352	—
Dy_{32}	5.20	384	—

properties listed in Table 3 indicate that Ag_{32} and Cu_{32} exhibit large HOMO–LUMO gaps, suggesting they may be the most stable isomers among the considered clusters that are ideal to be used for further studies. More importantly, even when their valence electron counts deviate from the traditional rule, elements such as Be, B, Si, and P can form stable O_h-symmetric clusters, as shown in Fig. 5(b). Among these, clusters like B_{32} and Be_{32} exhibit relatively large HOMO–LUMO gaps, indicating their enhanced electronic stability.

These findings significantly broaden our understanding of the factors governing the stability of fullerene-like clusters. They demonstrate that high-symmetry cage structures can be stabilized by elements beyond those satisfying conventional electron-counting rules, offering new pathways for the design of novel nanomaterials.

4. Conclusion

In this study, the structural properties and electronic properties of the Au_{32} fullerene clusters are deeply investigated through systematic theoretical calculations and structure optimizations. We found a new Au_{32} hollow cage fullerene structure with an O_h symmetry, which shows high stability in theoretical calculations; it has a relatively large HOMO–LUMO energy gap and exhibits excellent aromaticity, indicating its good thermodynamic and chemical stability. These findings not only enrich the understanding of the structural diversity of gold fullerene clusters but also provide a new theoretical basis for the stability of fullerene analogs. In addition, we successfully predicted the stable structures of the fullerene clusters of Au_{32}, Cu_{32}, B_{32}, and Si_{32} by populating them with all relevant elements. This study extend our understanding of the stability of fullerene-like compounds and provide new strategies for designing novel nanomaterials.

Conflicts of interest

There are no conflicts to declare.

Data availability

Supplementary information (SI) is available. See DOI: https://doi.org/10.1039/d5ra09961g.

Acknowledgements

This study was financially supported by the National Natural Science Foundation of China (No. 12274246 & 12534011). All the calculations were performed at the Supercomputing Center of Ningbo University and Ningbo Artificial Intelligence Supercomputing Center.

References

1 H. W. Kroto, J. R. Heath, S. C. O'Brien, R. F. Curl and R. E. Smalley, C_{60}: Buckminsterfullerene, *Nature*, 1985, **318**(6042), 162–163.
2 H. Selig, C. Lifshitz, T. Peres, J. E. Fischer, A. R. McGhie, W. J. Romanow, J. P. McCauley and A. B. Smith III, Fluorinated fullerenes, *Am. Chem. Soc.*, 1991, **113**(14), 5475–5476.
3 K. Kniaz, J. E. Fischer, H. Selig, G. B. M. Vaughan, W. J. Romanow, D. M. Cox, S. K. Chowdhury, J. P. McCauley, R. M. Strongin and A. B. Smith III, Fluorinated fullerenes: synthesis, structure, and properties, *Am. Chem. Soc.*, 1993, **115**(14), 6060–6064.
4 Y. F. Chang, J. P. Zhang, H. Sun, B. Hong, Z. An and R. S. Wang, Geometry and stability of fullerene cages: C_{24} to C_{70}, *Quantum Chem.*, 2005, **105**(2), 142–147.
5 N. Gonzalez Szwacki, A. Sadrzadeh and B. I. Yakobson, B_{80} fullerene: an ab initio prediction of geometry, stability, and electronic structure, *Phys. Rev. Lett.*, 2007, **98**(16), 166804.
6 G. Gopakumar, M. T. Nguyen and A. Ceulemans, The boron buckyball has an unexpected T_h symmetry, *Chem. Phys. Lett.*, 2008, **450**(4–6), 175–177.
7 N. Gonzalez Szwacki, Boron fullerenes: a first-principles study, *Nanoscale Res. Lett.*, 2008, **3**(2), 49–54.
8 L. Cheng, B_{14}: An all-boron fullerene, *J. Chem. Phys.*, 2012, **136**(10), 104301.
9 J. Lv, Y. Wang, L. Zhu and Y. Ma, B_{38}: an all-boron fullerene analogue, *Nanoscale*, 2014, **6**(20), 11692–11696.

10 J. Wang, T. Yu, Y. Gao and Z. Wang, All-boron fullerene B_{40}: a superatomic structure, *Sci. China Mater.*, 2017, **60**(12), 1264–1268.
11 H. J. Zhai, Y. F. Zhao, W. L. Li, Q. Chen, H. Bai, H. S. Hu, Z. A. Piazza, W. J. Tian, H. G. Lu and Y. B. Wu, Observation of an all-boron fullerene, *Nat. Chem.*, 2014, **6**(8), 727–731.
12 X. L. Sheng, Q. B. Yan, Q. R. Zheng and G. Su, Boron fullerenes $B_{32+\ 8k}$ with four-membered rings and B_{32} solid phases: geometrical structures and electronic properties, *Phys. Chem. Chem. Phys.*, 2009, **11**(42), 9696–9702.
13 S. Chopra, Boron fullerenes, B_n (n=20, 30, 38, 40, 50, 60): First principle calculations of electronic and optical properties, *J. Mol. Graphics Modell.*, 2018, **84**, 90–95.
14 L. Wang, J. Zhao, F. Li and Z. Chen, Boron fullerenes with 32–56 atoms: Irregular cage configurations and electronic properties, *Chem. Phys. Lett.*, 2010, **501**(1–3), 16–19.
15 C. Ozdogan, S. Mukhopadhyay, W. Hayami, Z. B. Guvenc, R. Pandey and I. Boustani, The unusually stable B_{100} fullerene, structural transitions in boron nanostructures, and a comparative study of α- and γ-boron and sheets, *J. Phys. Chem. C*, 2010, **114**(10), 4362–4375.
16 J. T. Muya, G. Gopakumar, M. T. Nguyen and A. Ceulemans, The leapfrog principle for boron fullerenes: a theoretical study of structure and stability of B_{112}, *Phys. Chem. Chem. Phys.*, 2011, **13**(16), 7524–7533.
17 X. Gu, M. Ji, S. H. Wei and X. G. Gong, Au_N clusters (N=32, 33, 34, 35): Cagelike structures of pure metal atoms, *Phys. Rev. B: Condens. Matter Mater. Phys.*, 2004, **70**(20), 205401.
18 J. P. Doye and D. J. Wales, Global minima for transition metal clusters described by Sutton–Chen potentials, *New J. Chem.*, 1998, **22**(7), 733–744.
19 J. Wang, J. Jellinek, J. Zhao, Z. Chen, R. B. King and P. von Rague Schleyer, Hollow cages versus space-filling structures for medium-sized gold clusters: the spherical aromaticity of the Au_{50} cage, *J. Phys. Chem. A*, 2005, **109**(41), 9265–9269.
20 W. Fa, J. Zhou, C. Luo and J. Dong, Cagelike Au_{32} detected in relativistic density-functional calculations of optical spectroscopy, *Phys. Rev. B: Condens. Matter Mater. Phys.*, 2006, **73**(8), 085405.
21 A. F. Jalbout, F. F. Contreras-Torres, L. A. Perez and I. L. Garzon, Low-symmetry structures of Au_{32}^{Z} (Z=+1, 0,−1) clusters, *J. Phys. Chem. A*, 2008, **112**(3), 353–357.
22 M. P. Johansson, J. Vaara and D. Sundholm, Exploring the stability of golden fullerenes, *J. Phys. Chem. C*, 2008, **112**(49), 19311–19315.
23 H. S. De, S. Krishnamurty and S. Pal, A first principle investigation on the thermal stability of a golden fullerene: A case study of Au_{32}, *Catal. Today*, 2012, **198**(1), 106–109.
24 F. Baletto and R. Ferrando, Doped golden fullerene cages, *Phys. Chem. Chem. Phys.*, 2015, **17**(42), 28256–28261.
25 L. X. Zhao, M. Zhang, H. Y. Zhang, X. J. Feng and Y. H. Luo, Unraveling Special Structures and Properties of Gold-Covered Gold-Core Cage on Au_{33-42} Nanoparticles, *J. Phys. Chem. A*, 2015, **119**(49), 11922–11927.
26 Q. Wang, J. F. Halet, S. Kahlal, A. Muñoz-Castro and J.-Y. Saillard, Electron count and electronic structure of bare icosahedral Au_{32} and Au_{33} ionic nanoclusters and ligated derivatives. Stable models with intermediate superatomic shell fillings, *Phys. Chem. Chem. Phys.*, 2020, **22**(36), 20751–20757.
27 K. Vishwanathan, $Au_{26\text{-}35}$: A special geometrical structure of Au_{33} (D_2) cluster with highly occupied-14 pairs of double-sate degeneracy, *Nanotechnology*, 2022, **16**, 063–080.
28 G. Kresse and J. Furthmüller, Efficient iterative schemes for ab initio total-energy calculations using a plane-wave basis set, *Phys. Rev. B: Condens. Matter Mater. Phys.*, 1996, **54**(16), 11169.
29 J. P. Perdew, K. Burke and M. Ernzerhof, Generalized gradient approximation made simple, *Phys. Rev. Lett.*, 1996, **77**(18), 3865–3868.
30 S. Grimme, J. Antony, S. Ehrlich and H. Krieg, A consistent and accurate ab initio parametrization of density functional dispersion correction (DFT-D) for the 94 elements H-Pu, *J. Chem. Phys.*, 2010, **132**(15), 154104.
31 P. E. Blochl, Projector augmented-wave method, *Phys. Rev. B: Condens. Matter Mater. Phys.*, 1994, **50**(24), 17953–17979.
32 D. Y. Zubarev and A. I. Boldyrev, Developing paradigms of chemical bonding: adaptive natural density partitioning, *Phys. Chem. Chem. Phys.*, 2008, **10**(34), 5207–5217.
33 M. J. Frisch, G. W. Trucks, H. B. Schlegel, G. E. Scuseria, M. A. Robb, J. R. Cheeseman, G. Scalmani, V. Barone, G. A. Petersson, H. Nakatsuji, X. Li, M. Caricato, A. V. Marenich, J. Bloino, B. G. Janesko, R. Gomperts, B. Mennucci, H. P. Hratchian, J. V. Ortiz, A. F. Izmaylov, J. L. Sonnenberg, D. Williams-Young, F. Ding, F. Lipparini, F. Egidi, J. Goings, B. Peng, A. Petrone, T. Henderson, D. Ranasinghe, V. G. Zakrzewski, J. Gao, N. Rega, G. Zheng, W. Liang, M. Hada, M. Ehara, K. Toyota, R. Fukuda, J. Hasegawa, M. Ishida, T. Nakajima, Y. Honda, O. Kitao, H. Nakai, T. Vreven, K. Throssell, J. A. Montgomery Jr, J. E. Peralta, F. Ogliaro, M. J. Bearpark, J. J. Heyd, E. N. Brothers, K. N. Kudin, V. N. Staroverov, T. A. Keith, R. Kobayashi, J. Normand, K. Raghavachari, A. P. Rendell, J. C. Burant, S. S. Iyengar, J. Tomasi, M. Cossi, J. M. Millam, M. Klene, C. Adamo, R. Cammi, J. W. Ochterski, R. L. Martin, K. Morokuma, O. Farkas, J. B. Foresman and D. J. Fox, *Gaussian 16 Rev. C.01*, Wallingford, CT, 2016.
34 T. Lu and F. Chen, Multiwfn: A multifunctional wavefunction analyzer, *J. Comput. Chem.*, 2012, **33**(5), 580–592.
35 T. Lu, A comprehensive electron wavefunction analysis toolbox for chemists, Multiwfn, *J. Chem. Phys.*, 2024, **161**(8), 082503.
36 P. Pyykko, Relativistic effects in structural chemistry, *Chem. Rev.*, 1988, **88**(3), 563–594.
37 P. Pyykkö, Theoretical chemistry of gold, *Angew. Chem., Int. Ed.*, 2004, **43**(34), 4412–4456.
38 P. Pyykkö, Theoretical chemistry of gold. II, *Inorg. Chim. Acta*, 2005, **358**(14), 4113–4130.

39 J. Li, X. Li, H.-J. Zhai and L.-S. Wang, Au_{20}: a tetrahedral cluster, *Science*, 2003, **299**(5608), 864–867.
40 Y. Gao and X. C. Zeng, Au_{42}: an alternative icosahedral golden fullerene cage, *Am. Chem. Soc.*, 2005, **127**(11), 3698–3699.
41 A. Muñoz-Castro, D_{6h}-Au_{42} Isomer: A Golden Aromatic Toroid Involving Superatomic π-Orbitals that Follow the Hückel (4n+2)π rule, *ChemPhysChem*, 2016, **17**(20), 3204–3208.
42 S. Bulusu, X. Li, L. S. Wang and X. C. Zeng, Evidence of hollow golden cages, *Proc. Natl. Acad. Sci. U. S. A.*, 2006, **103**(22), 8326–8330.
43 A. Lechtken, D. Schooss, J. R. Stairs, M. N. Blom, F. Furche, N. Morgner, O. Kostko, B. von Issendorff and M. M. Kappes, Au_{34}^-: a chiral gold cluster?, *Angew. Chem., Int. Ed.*, 2007, **46**(16), 2944–2948.
44 D. Tian, J. Zhao, B. Wang and R. B. King, Dual relationship between large gold clusters (antifullerenes) and carbon fullerenes: a new lowest-energy cage structure for Au_{50}, *J. Phys. Chem. A*, 2007, **111**(3), 411–414.
45 J. M. Jacobo-Fernández and A. Tlahuice-Flores, Effect of the charge state on the structure of the Au_{60} cluster, *Phys. Chem. Chem. Phys.*, 2021, **23**(1), 442–448.
46 A. J. Karttunen, M. Linnolahti, T. A. Pakkanen and P. Pyykkö, Icosahedral Au_{72}: a predicted chiral and spherically aromatic golden fullerene, *Chem. Commun.*, 2008, (4), 465–467.
47 H. Ning, J. Wang, Q. M. Ma, H. Y. Han and Y. Liu, A series of quasi-icosahedral gold fullerene cages: Structures and stability, *Phys. Chem. Solids*, 2014, **75**(5), 696–699.
48 C. D. Dong and X. G. Gong, Gold cluster beyond hollow cage: A double shell structure of Au_{58}, *J. Chem. Phys.*, 2010, **132**(10), 104301.
49 P. Pyykkö, Theoretical chemistry of gold. III, *Chem. Soc. Rev.*, 2008, **37**(9), 1967–1997.
50 A. Tlahuice-Flores, New Polyhedra Approach To Explain the Structure and Evolution on Size of Thiolated Gold Clusters, *J. Phys. Chem. C*, 2019, **123**(17), 10831–10841.
51 S. L. Wang, J. Tian, J. Y. Li, T. Gong, X. Yan, J. J. Zhao, X. G. Gong and X. Gu, Conjugate-dual clusters, *J. Chem. Phys.*, 2025, **163**(7), 074303.
52 Z. Jun and D. Michael, ABCluster: the artificial bee colony algorithm for cluster global optimization, *Phys. Chem. Chem. Phys.*, 2015, **17**(37), 24173–24181.
53 M. Ji, X. Gu, X. Li, X. G. Gong, J. Li and L. S. Wang, Experimental and theoretical investigation of the electronic and geometrical structures of the Au_{32} cluster, *Angew. Chem., Int. Ed.*, 2005, **44**(43), 7119–7123.
54 S. Darby, T. V. Mortimer-Jones, R. L. Johnston and C. Roberts, Theoretical study of Cu–Au nanoalloy clusters using a genetic algorithm, *J. Chem. Phys.*, 2002, **116**(4), 1536–1550.
55 M. Itoh, V. Kumar, T. Adschiri and Y. Kawazoe, Comprehensive study of sodium, copper, and silver clusters over a wide range of sizes 2≤N≤75, *J. Chem. Phys.*, 2009, **131**(17), 174510–174511.
56 S. Nunez and R. L. Johnston, Structures and Chemical Ordering of Small Cu-Ag Clusters, *J. Phys. Chem. C*, 2010, **114**(31), 13255–13266.
57 D. Michael and P. Mingo, Polyhedral skeletal electron pair approach, *Acc. Chem. Res.*, 1984, **17**(9), 311–319.
58 M. Darvish Ganji, H. Tavassoli Larijani, R. Alamol-hoda and M. Mehdizadeh, First-principles and Molecular Dynamics simulation studies of functionalization of Au32 golden fullerene with amino acids, *Sci. Rep.*, 2018, **8**(1), 11400.
59 S. F. Yuan, C. Q. Xu, J. Li and Q. M. Wang, A Ligand-Protected Golden Fullerene: The Dipyridylamido Au328+ Nanocluster, *Angew. Chem., Int. Ed.*, 2019, **58**(18), 5906–5909.
60 J. Ye, Y. Dai, W. Liu, J. Xu, J. Li, M. Chen, S. Yang, Q. Li, Y. Du, J. Chai and M. Zhu, Phosphine-induced conversion from Au36 to Au32 for constructing a high-performance CO2RR catalyst, *Dalton Trans.*, 2025, **54**(23), 9160–9168.